For RNA transfection, the cells were washed with phosphate-buffered saline (PBS) and resuspended in complete growth medium. The cells were then pelleted by centrifugation (1,400 × *g* for 4 min at 4°C), washed twice with ice-cold PBS, and resuspended in ice-cold PBS at a concentration of 7.5×10^6 cells/0.4 ml. The cells were mixed with 10 μg of the RNA transcripts, placed into 2-mm-gap electroporation cuvettes (BTX Genetronics, San Diego, CA), and electroporated with five pulses of 99 μs at 750 V over 1.1 s in an ECM 830 (BTX Genetronics). Following a 10-min recovery period, the cells were mixed with complete growth medium and plated.

miR-27a and anti-miR-27a transfection. Huh-7.5 cells transfected with pH77Sv2 Gluc2A RNA or pH77Sv2 Gluc2A (AAG) RNA were transfected with 50 nM synthetic miRNA (pre-miRNA) or 50 nM anti-miRNA (Ambion Inc., Austin, TX) with the siPORTTM NeoFXTM Transfection Agent (Ambion). Transfection was performed immediately by mixing the electroporated cells with the miRNA transfection reagents. Control samples were transfected with an equal concentration of a nontargeting control (pre-miRNA negative control) or inhibitor negative control (anti-miRNA negative control) to assess non-sequence-specific effects in the miRNA experiments.

Fatty acid treatment. Huh-7.5 cells transfected with HCV RNA and pre- or anti-miRNA were cultured for 24 h and then treated with the indicated concentrations of oleic acid (0 to 250 μM) (26) in the presence of 2% free fatty acid (FFA)-free bovine serum albumin (BSA; Sigma-Aldrich, St. Louis, MO). The cells were harvested at 72 h posttreatment with oleic acid for quantitative real-time detection PCR (RTD-PCR), Western blotting, immunofluorescence staining, and reporter analysis. The number of viable cells was determined by an MTS assay [one-step 3-(4,5-dimethylthiazol-2-yl)-2,5-diphenyltetrazolium bromide assay; Promega Corporation, Madison, WI]. Cellular triglyceride (TG) and cholesterol (TCHO) contents were measured with TG Test Wako and Cholesterol Test Wako kits (Wako, Osaka, Japan) according to the manufacturer's instructions.

Equilibrium ultracentrifugation of JFH-1 particles in isopycnic iodixanol gradients. Filtered supernatant fluids collected from JFH-1 RNA- and pre-miRNA- or anti-miRNA-transfected cell cultures were concentrated 30-fold with a Centricon PBHK Centrifugal Plus-20 filter unit with an Ultracel PL membrane (100-kDa exclusion; Merck Millipore, Billerica, MA) and then layered on top of a preformed continuous 10 to 40% iodixanol (OptiPrep; Sigma-Aldrich) gradient in Hanks' balanced salt solution (Invitrogen, Carlsbad, CA) as described previously (24). The gradients were centrifuged in an SW41 rotor (Beckman Coulter Inc., Brea, CA) at 35,000 rpm for 16 h at 4°C, and the fractions (500 μl each) were collected from the top of the tube. The density of each fraction was determined with a digital refractometer (Atago, Tokyo, Japan).

Infectivity assays. Huh-7.5 cells were seeded at 5.0×10^4/well in 48-well plates 24 h before inoculation with 100 μl of the gradient fractions. The cells were tested for the presence of intracellular core antigen by immunofluorescence 72 h later, as described below. Clusters of infected cells that stained for the core antigen were considered to constitute a single infectious focus, and virus titers were calculated accordingly in terms of numbers of focus-forming units (FFU)/ml.

Western blotting and immunofluorescence staining. Western blotting was performed as described previously (27). The cells were washed in PBS and lysed in radioimmunoprecipitation assay buffer containing Complete protease inhibitor cocktail and PhosSTOP (Roche Applied Science, Indianapolis, IN). The membranes were blocked in Blocking One or Blocking One-P solution (Nacalai Tesque, Kyoto, Japan), and the expression of HCV core protein, retinoid X receptor alpha (RXRα), sterol regulatory element-binding protein (SREBP1), ATP-binding cassette subfamily A member 1 (ABCA1), ApoE3, ApoB100, fatty acid synthase (FASN), peroxisome proliferator-activated receptor α (PPARα), ApoA1, phospho-PKR-like ER kinase (phospho-PERK), PERK, phospho-eIF2α, eIF2α, BIP, phospho-STAT1, and β-actin was evaluated with mouse anti-core (Thermo Fisher Scientific Inc., Rockford, IL), rabbit anti-RXRα, rabbit anti-SREBP1 (Santa Cruz Biotechnology Inc., Santa Cruz, CA), mouse anti-ABCA1 (Abcam, Cambridge, MA), goat anti-ApoE3, goat anti-ApoB100 (R&D Systems Inc., Minneapolis, MN), rabbit anti-FASN, rabbit anti-PPARα, mouse anti-ApoA1, rabbit anti-phospho-PERK, rabbit anti-PERK, rabbit anti-phospho-eIF2α, rabbit anti-eIF2α, rabbit anti-BIP, rabbit anti-phospho-STAT1, and rabbit anti-β-actin antibodies (Cell Signaling Technology Inc., Danvers, MA), respectively.

For immunofluorescence staining, the cells were washed twice with PBS and fixed in 4% paraformaldehyde for 15 min at room temperature. After washing again with PBS, the cells were permeabilized with 0.05% Triton X-100 in PBS for 15 min at room temperature. They were then incubated in a blocking solution (10% FBS and 5% BSA in PBS) for 30 min and with the anti-core monoclonal antibodies. The fluorescent secondary antibodies were Alexa 568-conjugated anti-mouse IgG antibodies (Invitrogen). Nuclei were labeled with 4′,6-diamidino-2-phenylindole (DAPI), and LDs were visualized with boron-dipyrromethene (BODIPY) 493/503 (Invitrogen). Imaging was performed with a CSU-X1 confocal microscope (Yokogawa Electric Corporation, Tokyo, Japan).

Quantitative RTD-PCR. Total RNA was isolated with a GenElute Mammalian Total RNA Miniprep kit (Sigma-Aldrich), and cDNA was synthesized with a high-capacity cDNA reverse transcription kit (Applied Biosystems, Carlsbad, CA). The primer pairs and probes for C/EBPα, ABCA1, PPARγ, SREBF1, SREBF2, FASN, 2′-5′-oligoadenylate synthetase 2 (OAS2), and β-actin were obtained from the TaqMan assay reagent library. HCV RNA was detected as described previously (28). HCV RNA was isolated from viral particles with a QIAamp viral RNA kit (Qiagen, Inc., Valencia, CA) in accordance with the manufacturer's instructions. Total RNA containing miRNA was isolated according to the protocol of the mirVana miRNA isolation kit (Ambion). For the enrichment of mature miRNA, argonaute 2 (Ago2)-binding miRNA was immunoprecipitated with an anti-Ago2 monoclonal antibody (Wako) and mature miRNA was eluted from the precipitant with a microRNA isolation kit, Human Ago2 (Wako). cDNA was prepared via reverse transcription with 10 ng of isolated total RNA and 3 μl of each reverse transcription primer with specific loop structures. Reverse transcription was performed with a TaqMan MicroRNA reverse transcription kit (Applied Biosystems) according to the manufacturer's protocol. RTD-PCR was performed with the 7500 Real Time PCR system (Applied Biosystems) according to the manufacturer's instructions. The primer pairs and probes for miR-let7a, miR-34c, miR-142-5p, miR-27a, miR-23a, and RNU6B were obtained from the TaqMan assay reagent library.

3′ UTR luciferase reporter assays. The miRNA expression reporter vector pmirGLO Dual-Luciferase miRNA Target Expression Vector (Promega Corporation) was used to validate the RXRα and ABCA1 3′ untranslated regions (UTRs) as miRNA binding sites. cDNA fragments corresponding to the entire 3′ UTR of human RXRα and human ABCA1 were amplified with the Access RT-PCR system (Promega Corporation) from total RNA extracted from Huh-7.5 cells. The PCR products were cloned into the designated multiple cloning site downstream of the luciferase open reading frame between the SacI and XhoI restriction sites of the pCR2.1-TOPO vector (Invitrogen). Point mutations in the seed region of the predicted miR-27a sites within the 3′ UTR of human RXRα and human ABCA1 were generated with a QuikChange Multi site-directed mutagenesis kit (Agilent Technologies Inc., Santa Clara, CA) according to the manufacturer's protocol. All constructs were confirmed by sequencing.

Huh-7.5 cells were grown to 70% confluence in 24-well plates in complete DMEM. The cells were cotransfected with 200 ng of the indicated 3′ UTR luciferase reporter vector and 50 nM synthetic miRNA (pre-miRNA) or 50 nM anti-miRNA (Ambion) in a final volume of 0.5 ml with Lipofectamine 2000 (Invitrogen). At 24 h posttransfection, firefly and *Renilla* luciferase activities were measured consecutively with the Dual-Luciferase Reporter Assay system (Promega Corporation).

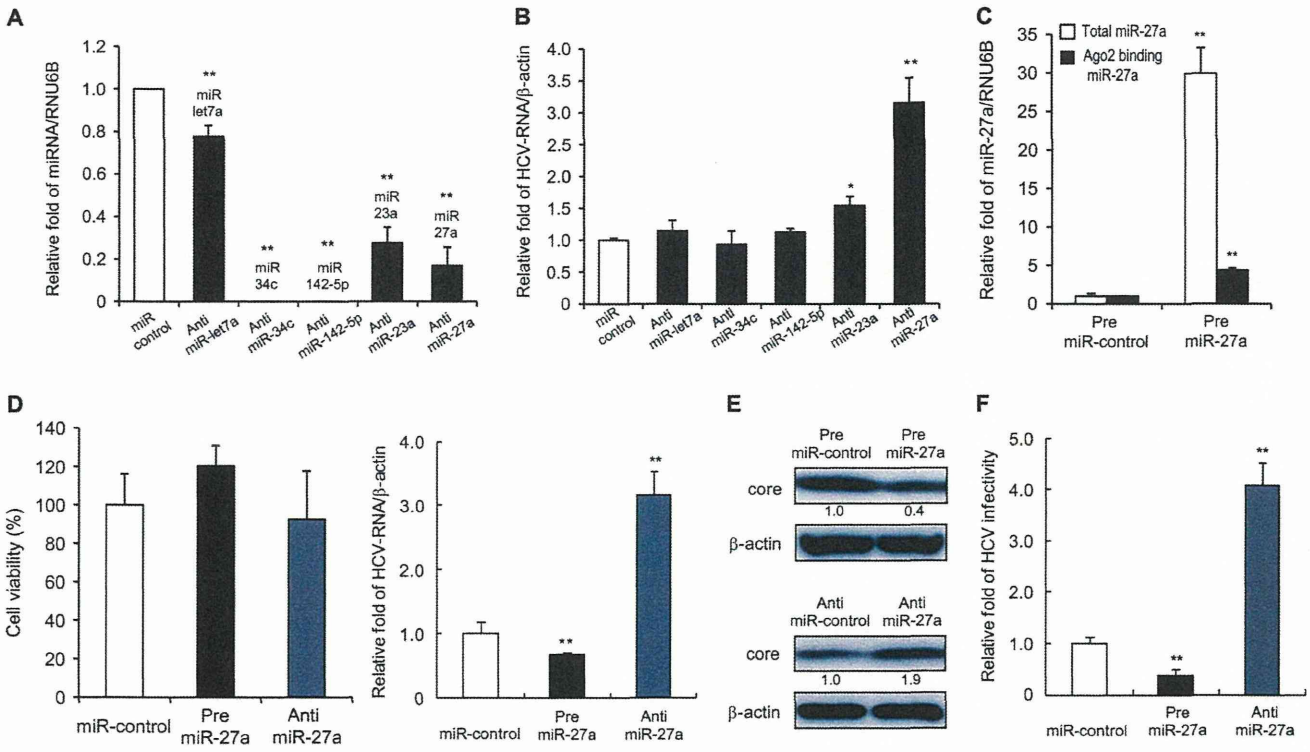

FIG 1 miR-27a has a negative effect on HCV replication and infectivity. Huh-7.5 cells were transfected with JFH-1 RNA and pre- or anti-miRNA. Expression was quantified at 72 h posttransfection. (A) Inhibition efficiency of miRNAs by anti-miRNAs (RTD-PCR, $n = 6$). (B) Effects of anti-miRNAs on HCV replication (RTD-PCR, $n = 6$). (C) Detection of whole miR-27a and Ago2-binding miR-27a in Huh-7.5 cells. At 72 h posttransfection, cells were harvested and Ago2-binding miRNA was purified as described in Materials and Methods. White bars indicate total miR-27a levels, and black bars indicate Ago2-binding miR-27a levels (RTD-PCR, $n = 6$). (D) Effects of pre- or anti-miR-27a on cell viability (left) and HCV replication (right). Cell viability (%) was assessed by the MTS assay ($n = 6$). (E) Effects of pre- or anti-miR-27a on HCV core protein levels by Western blotting. (F) Effects of pre- or anti-miR-27a on HCV infection. Huh-7.5 cells were infected with HCVcc derived from Huh-7.5 cells transfected with pre- or anti-miR-27a and JFH-1 RNA. HCV RNA was quantified at 72 h postinfection by RTD-PCR ($n = 6$). All experiments were performed in duplicate and repeated three times. Values are means ± standard errors. *, $P < 0.01$; **, $P < 0.005$.

Promoter analysis. DNA fragments from −400 to +36 bp and from −700 to +36 bp relative to the transcription initiation site of pri-miR-23a~27a~24-2 were inserted into pGL3-Basic (Promega Corporation) at the MluI and XhoI sites. Point mutations in the seed region of predicted C/EBPα binding sites were generated with a QuikChange Multi site-directed mutagenesis kit (Agilent Technologies) according to the manufacturer's protocol. All constructs were confirmed by sequencing.

Huh-7.5 cells transfected with HCV RNA were cultured for 24 h in 24-well plates, and then 200 ng of the plasmids was cotransfected with 2 ng of the *Renilla* luciferase expression vector (pSV40-Renilla) with the FuGENE6 Transfection Reagent (Roche Applied Science). After 24 h, the cells were treated with oleic acid in the presence of 2% FFA-free BSA (Sigma-Aldrich). At 48 h posttreatment, a luciferase assay was carried out with the Dual-Luciferase Reporter Assay system (Promega Corporation) according to the manufacturer's instructions.

For tunicamycin treatment, the plasmids (200 ng) were cotransfected with 2 ng pSV40-Renilla with FuGENE6 (Roche Applied Science) into Huh-7.5 cells grown in the wells of 24-well plates. After 24 h, the cells were treated for a further 24 h with the indicated concentrations of tunicamycin and a luciferase assay was carried out as described above.

RNA interference. A small interfering RNA (siRNA) specific to ABCA1 and a control siRNA were obtained from Thermo Fisher Scientific. Transfection was performed with Lipofectamine 2000 (Invitrogen) according to the manufacturer's instructions.

IFN treatment. Huh-7.5 cells transfected with HCV RNA and pre- or anti-miRNA were treated with oleic acid as described above. At 48 h later, the cells were treated with the indicated number of international units of IFN-α for 24 h.

Affymetrix GeneChip analysis. Aliquots of total RNA (50 ng) isolated from the cells were subjected to amplification with the WT-Ovation Pico RNA Amplification system (NuGen, San Carlos, CA) according to the manufacturer's instructions. The Affymetrix Human U133 Plus 2.0 microarray chip containing 54,675 probes has been described previously (29).

Statistical analysis. Results are expressed as mean values ± standard errors. At least six samples were tested in each assay. Significance was tested by one-way analysis of variance with Bonferroni methods, and differences were considered statistically significant at P values of <0.01 (*, $P < 0.01$; **, $P < 0.005$).

Microarray accession number. The expression data determined in this study were deposited in the Gene Expression Omnibus database (NCBI) under accession number GSE41737.

RESULTS

Functional relevance of the upregulated miRNAs in HCV-infected livers. Previously, 19 miRNAs were shown to be differentially expressed in HBV- and HCV-infected livers (2). Of these, 6 miRNAs were upregulated and 13 were downregulated. In this study, we focused on the upregulated miRNAs, as they might play a positive role in HCV replication. Anti-miRNAs and the control miRNA were transfected into Huh-7.5 cells following JFH-1 RNA

TABLE 1 Gene categories and names of differentially expressed genes regulated by miR-27a in Huh-7.5 cells

Protein function and name	Gene	Affy ID[a]	GB acc. no.[b]	Fold change		
				Pre-miR-27a/ miR-control	Anti-miR-27a/ anti-miR-control	Pre-miR-27a/ anti-miR-27a
Cytoskeleton remodeling and Wnt signaling						
Collagen, type IV, alpha 6	*COL4A6*	211473_s_at	U04845	0.85	2.19	2.58
Fibronectin 1	*FN1*	214702_at	AJ276395	0.57	1.14	2.02
Filamin A, alpha	*FLNA*	214752_x_at	AI625550	0.64	1.68	2.61
LIM domain kinase 1	*LIMK1*	204357_s_at	NM_002314	0.67	1.63	2.43
p21/Cdc42/Rac1-activated kinase 1	*PAK1*	230100_x_at	AU147145	0.63	1.58	2.53
Breast cancer anti-estrogen resistance 1	*BCAR1*	232442_at	AU147442	0.96	1.94	2.01
Frizzled homolog 3 (*Drosophila*)	*FZD3*	219683_at	NM_017412	0.51	1.30	2.55
Laminin, alpha 4	*LAMA4*	210990_s_at	U77706	0.63	1.26	2.00
Regulation of lipid metabolism						
CREB binding protein (Rubinstein-Taybi syndrome)	*CREBBP*	235858_at	BF507909	0.54	1.50	2.76
NF-Y	*NF-Y*	228431_at	AL137443	0.41	1.44	3.50
Sterol regulatory element binding transcription factor 2	*SREBF2*	242748_at	AA112403	0.47	1.11	2.35
Membrane-bound transcription factor peptidase, site 2	*MBTPS2*	1554604_at	BC036465	0.50	1.21	2.39
Adenosine A2A receptor signaling						
Mitogen-activated protein kinase kinase 7	*MAP2K7*	226053_at	AI090153	0.90	2.07	2.31
Par-6 partitioning defective 6 homolog beta	*PARD6B*	235165_at	AW151704	0.56	1.35	2.43
Rap guanine nucleotide exchange factor (GEF) 2	*RAPGEF2*	238176_at	T86196	0.46	1.36	2.98
Ribosomal protein S6 kinase, 90kDa, polypeptide 2	*RPS6KA2*	204906_at	BC002363	0.61	1.72	2.83
p53 regulation						
MDM2	*MDM2*	237891_at	AI274906	0.41	1.27	3.07
Ubiquitin B	*UBB*	217144_at	X04801	0.58	1.89	3.24
Promyelocytic leukemia	*PML*	235508_at	AW291023	0.52	1.45	2.80
SMT3 suppressor of mif two 3 homolog 1	*SUMO1*	208762_at	U83117	0.55	1.23	2.22
IL-8 in angiogenesis						
B-cell CLL/lymphoma 10	*BCL10*	1557257_at	AA994334	0.59	1.23	2.08
Janus kinase 2	*JAK2*	205841_at	NM_004972	0.77	1.71	2.23
Sphingosine-1-phosphate receptor 1						
G protein, alpha inhibiting activity polypeptide 2	*GNAI2*	201040_at	NM_002070	0.69	1.49	2.15
G protein, beta polypeptide 4	*GNB4*	223487_x_at	AW504458	0.86	1.78	2.06
Mitogen-activated protein kinase 1	*MAPK1*	1552263_at	NM_138957	0.87	1.93	2.22
GRB2-associated binding protein 1	*GAB1*	226002_at	AK022142	0.66	1.40	2.11

[a] Affy ID, Affymetrix identification number.
[b] GB acc. no., GenBank accession number.

transfection. The efficiency with which these anti-miRNAs inhibit the miRNAs is shown in Fig. 1A. Unexpectedly, inhibition of these miRNAs either had no effect or increased HCV replication in the cases of anti-miR-23a and anti-miR-27a (Fig. 1B).

To investigate the functional relevance of miR-27a in HCV replication in more detail, we evaluated JFH-1 replication in Huh-7.5 cells in which miR-27a was inhibited or overexpressed. The efficacy of miR-27a overexpression is shown in Fig. 1C. Although ectopically introduced pre-miR-27a increased miR-27a levels by approximately 30-fold, the levels of endogenous active Ago2 bound to miR-27a in RNA-induced silencing complexes increased by approximately 5-fold. The RNA and core protein levels of JFH-1 in Huh-7.5 cells decreased to 65% and 40%, respectively, following miR-27a overexpression. In contrast, the RNA and core protein levels of JFH-1 increased by 3- and 1.9-fold, respectively, following miR-27a inhibition (Fig. 1D and E). There was no significant difference in cell viability following miR-27a overexpression or inhibition (Fig. 1D). Furthermore, the rate of Huh-7.5 cell infection by JFH-1 decreased to 35% after the overexpression of miR-27a but increased 4-fold after miR-27a inhibition (Fig. 1F). Thus, miR-27a negatively regulates HCV replication and infection.

miR-27a targets the signaling pathways of cytoskeleton remodeling and lipid metabolism in Huh-7.5 cells. We next examined which signaling pathways were modulated by miR-27a. TargetScan (http://www.targetscan.org/) predicts biological targets of miRNAs by searching for the presence of conserved 8- and 7-mer sites that match the seed region of each miRNA (30). A TargetScan (release 5.2) for miR-27a predicted 921 candidate target genes, and functional gene ontology enrichment analysis of these genes by MetaCore (Thomson Reuters, New York, NY) showed that miR-27a could target the cytoskeleton remodeling and lipid metabolism signaling pathways (data not shown).

To examine whether these signaling pathways were regulated by miR-27a, gene expression profiling was carried out with Huh-7.5 cells in which miR-27a was over- or underexpressed. Transfection of cells with pre-miR-27a and pre-miR-

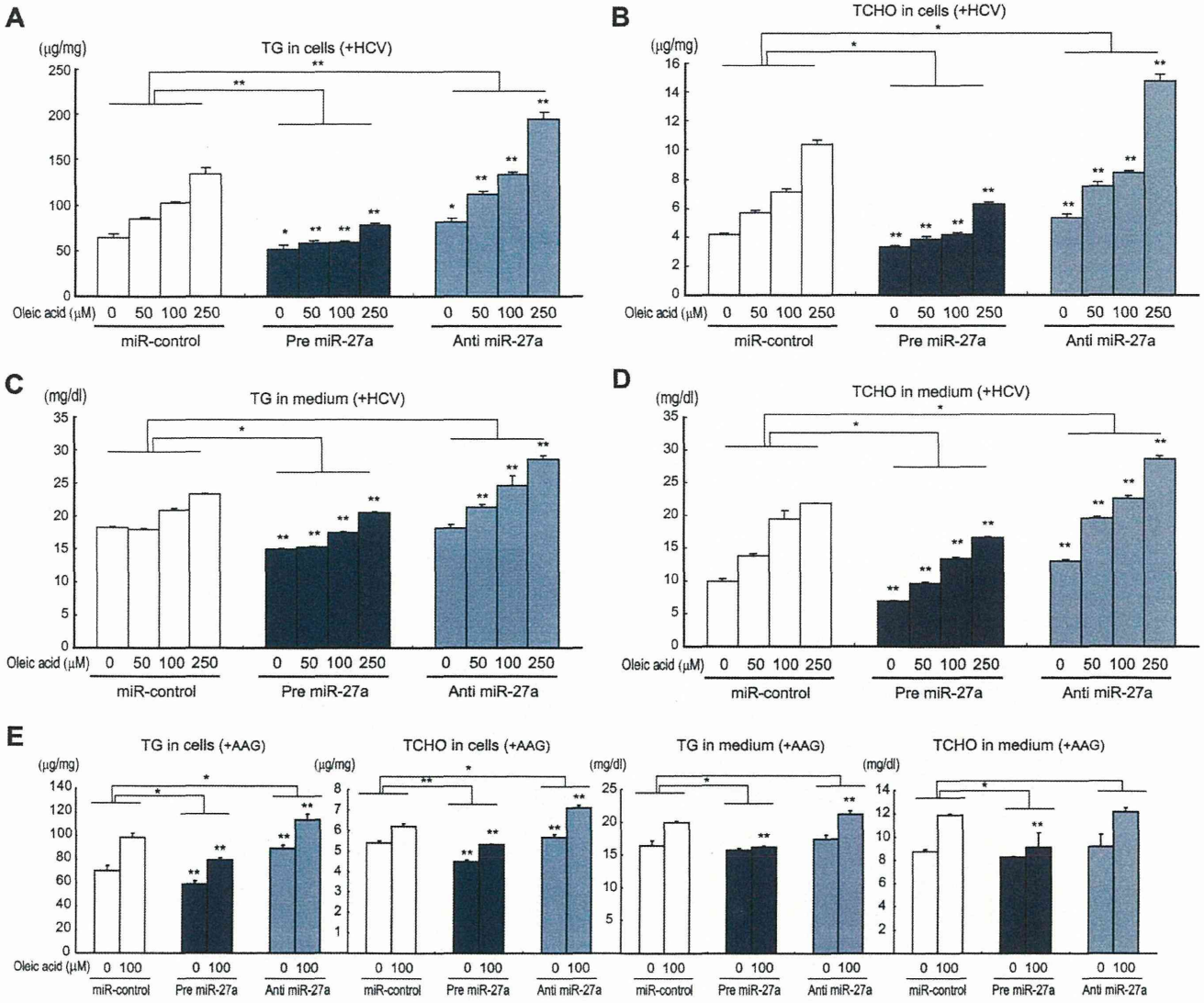

FIG 2 Changes in the lipid contents of Huh-7.5 cells and culture medium caused by pre- and anti-miR-27a. Huh-7.5 cells were transfected with replication-competent HCV RNA (H77Sv2 Gluc2A RNA [+HCV]) or replication-incompetent HCV RNA [H77Sv2 Gluc2A (AAG) (+AAG)] together with pre- or anti-miR-27a. At 24 h posttransfection, increasing amounts of oleic acid (0 to 250 μM) were added to the culture medium, and at 72 h after oleic acid treatment, TG and TCHO levels were measured in the cells and medium. Panels: A, TG in cells; B, TCHO in cells; C, TG in medium; D, TCHO in medium; E, TG and TCHO in cells and medium; A to D, +H77Sv2 Gluc2A (+HCV); E, +H77Sv2 Gluc2A (AAG) (+AAG). Lipid concentration was compared with that of miR-control and pre- or anti-miRNA ($n = 6$). All experiments were performed in duplicate and repeated three times. Values are means ± standard errors. *, $P < 0.01$; **, $P < 0.005$.

control or with anti-miR-27a and anti-miR-control enabled the identification of down- and upregulated genes, respectively. A total of 870 genes were selected with a >2-fold anti-miR-27a/pre-miR-27a expression ratio. Pathway analysis of these genes with MetaCore revealed that they are involved in cytoskeleton remodeling signaling, including that of *COL4A6*, *FN 1*, and *PAK1*; lipid metabolism signaling, including that of *CREBBP* and *SREBF2*; A2A receptor signaling, including that of *RAPGEF2*; and p53 regulation signaling, including that of *MDM2*. These genes were repressed by miR-27a in Huh-7.5 cells (Table 1).

miR-27a reduces TG and TCHO levels in cells and culture medium. Pathway analysis of the gene expression profile regulated by miR-27a in Huh-7.5 cells revealed the presence of many genes involved in lipid metabolism-related signaling pathways. To examine the functional relevance of miR-27a in lipid metabolism, we measured the cellular levels of TG and TCHO in Huh-7.5 cells in which miR-27a was inhibited or overexpressed, respectively. As shown in Fig. 2A and B, TG and TCHO levels in Huh-7.5 cells transfected with miR-control were increased in a dose-dependent manner following the addition of oleic acid (0 to 250 μM). Pre-miR-27a repressed this increase, while anti-miR-27a significantly accelerated it. Similarly, pre-miR-27a repressed the increase in TG and TCHO in the culture medium, while anti-miR-27a significantly accelerated it (Fig. 2C and D).

Similar results were obtained with both HCV-replicating cells

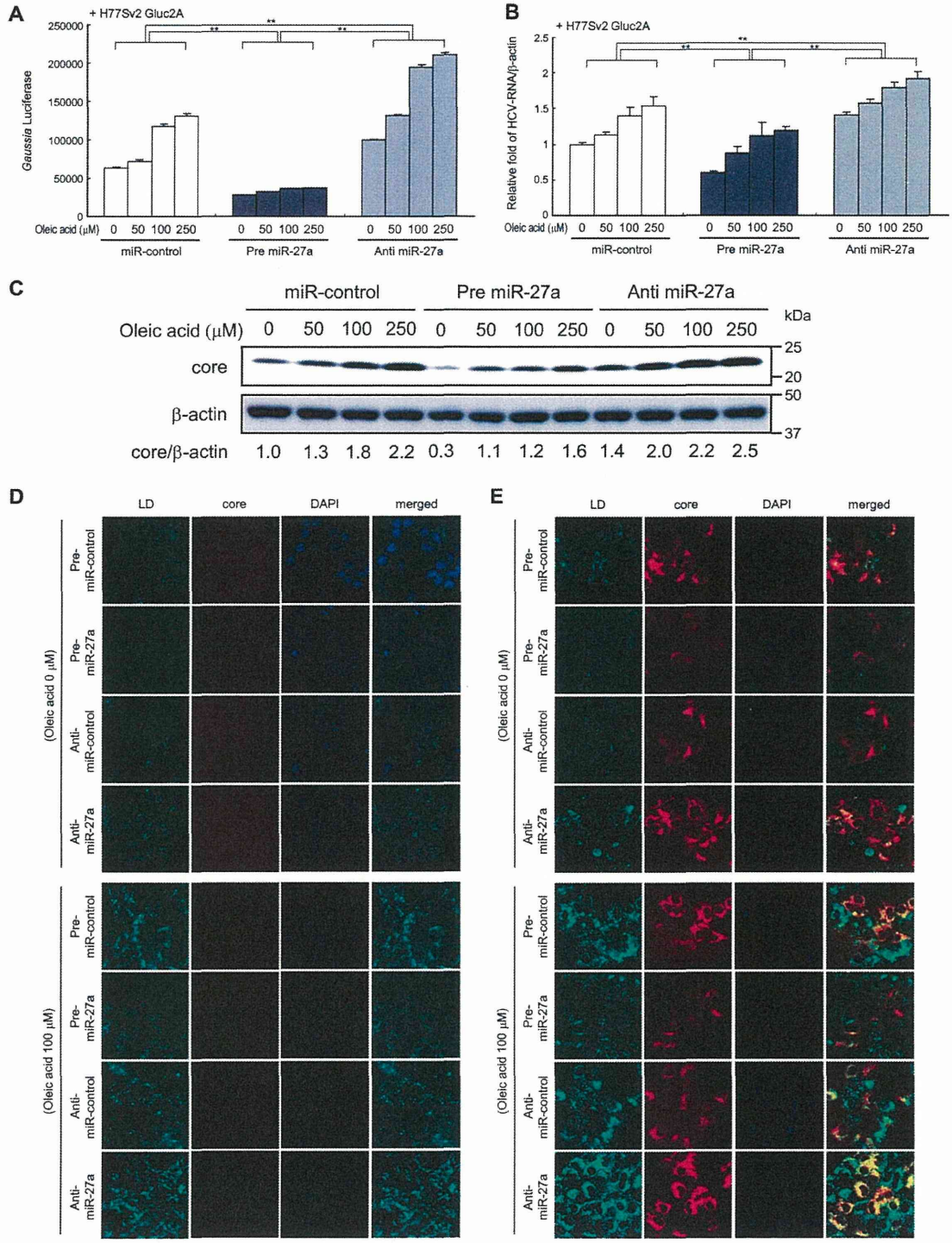

FIG 3 Changes in HCV replication in Huh-7.5 cells caused by pre- and anti-miR-27. Huh-7.5 cells were transfected with H77Sv2 Gluc2A RNA or H77Sv2 Gluc2A (AAG) RNA and pre- or anti-miR-27a. At 24 h posttransfection, increasing amounts of oleic acid (0 to 250 μM) were added to the culture medium. At 72 h after oleic acid treatment, the cells were harvested. (A) Gluc activity in the medium reflecting HCV replication in cells ($n = 6$). (B) Effects of pre- or anti-miR-27 on HCV RNA levels (RTD-PCR, $n = 6$). Experiments were performed in duplicate and repeated three times. Values are means ± standard errors. *, $P < 0.01$; **, $P < 0.005$. (C) Western blotting of HCV core protein in the same experiments. (D and E) Confocal microscopy images of Huh-7.5 cells in the same experiments. D, +H77Sv2 Gluc2A (AAG); E, +H77Sv2 Gluc2A. Cells were fixed, permeabilized, and stained with an anti-HCV core protein antibody. Nuclei were labeled with DAPI. LDs were visualized with BODIPY 493/503 dye. Imaging was performed with a CSU-X1 confocal microscope.

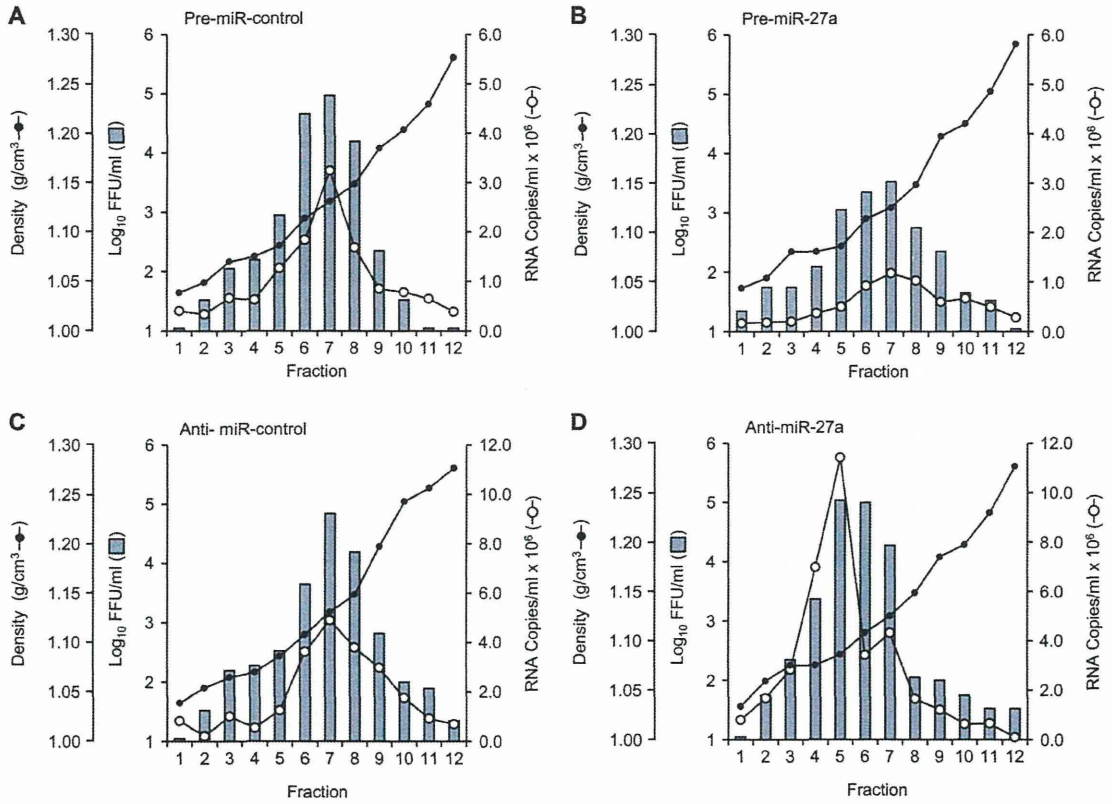

FIG 4 Equilibrium ultracentrifugation of JFH-1 particles in isopycnic iodixanol gradients. Filtered supernatant fluids collected from JFH-1 RNA- and pre- or anti-miRNA-transfected Huh-7.5 cell cultures were concentrated and used to collect fractions (500 μl each). Black circles indicate the gradient densities of the fractions, white circles indicate the HCV RNA titers, and bars indicate HCV infectivity levels. Panels: A, cells overexpressing pre-miR-control; B, cells overexpressing pre-miR-27a; C, cells overexpressing anti-miR-control; D, cells overexpressing anti-miR-27a. Experiments were repeated twice.

(+HCV) (Fig. 2A to D) and non-HCV-replicating cells (+AAG) (Fig. 2E), although the changes in the levels of TG and TCHO in the culture medium were smaller for the non-HCV-replicating cells (+AAG) (Fig. 2E). Correlating with the lipid component findings, replication of the infectious HCV clone H77Sv2 Gluc2A (21), as determined by Gluc activity in the culture medium, and the HCV RNA titer were significantly repressed by pre-miR-27a and increased by anti-miR-27a (Fig. 3A and B). This result was also confirmed by the core protein levels determined by Western blotting (Fig. 3C).

The localization of LDs and core proteins in the cells was visualized by confocal laser microscopy with a lipotropic fluorescent dye and immunostaining of the core protein (Fig. 3E). The LD and core protein levels were substantially repressed by pre-miR-27a and greatly increased by anti-miR-27a antibody. The change in the levels of LDs caused by miR-27a was observed in both HCV-replicating cells (Fig. 3E) and non-HCV-replicating cells (Fig. 3D), although the magnitude of the change was more prominent in HCV-replicating cells.

miR-27a changes the buoyant density and infectivity of HCV particles. The culture medium of Huh-7.5 cells in which JFH-1 was replicating was fractionated by iodixanol gradient centrifugation, and the buoyant density of HCV particles was evaluated (Fig. 4). When the cells were transfected with control miRNA (pre-miR-control and anti-miR-control), the HCV RNA titer (number of copies/ml) and infectivity (number of FFU/ml) peaked at fraction 7 (Fig. 4A and D) and the buoyant density of HCV was estimated at around 1.13 g/cm^3. Transfection with pre-miR-27a did not change the buoyant density of HCV, but it reduced the HCV RNA titer to 0.25-fold of the control and HCV infectivity to 0.024-fold of the control (Fig. 4B). In contrast, transfection with anti-miR-27a reduced the buoyant density of HCV from 1.13 to 1.08 g/cm^3 (Fig. 4B) and increased the HCV RNA titer to 2.1-fold of the control and infectivity to 2.5-fold of the control (Fig. 4C and D). Thus, miR-27a changed the buoyant density and infectivity of HCV.

miR-27a regulates lipid metabolism-related gene expression. The regulation of lipid metabolism-related genes by miR-27a was evaluated in Huh-7.5 cells (Fig. 5 and 6). The lipid synthesis transcription factors PPARγ, FASN, SREBP1, SREBP2, and RXRα were slightly, but significantly, induced in cells in which H77Sv2 Gluc2A replicated. The expression of lipid synthesis transcription factors was compared with that from cells carrying replication-incompetent H77Sv2 Gluc2A (AAG) (Fig. 5 and 6). Unexpectedly, lipid overload with oleic acid had no effect or rather decreased the levels of these transcription factors in non-HCV-replicating cells, probably because of negative feedback mechanisms. Conversely, in HCV-replicating cells, lipid overload with oleic acid further increased the levels of these transcription factors at both the

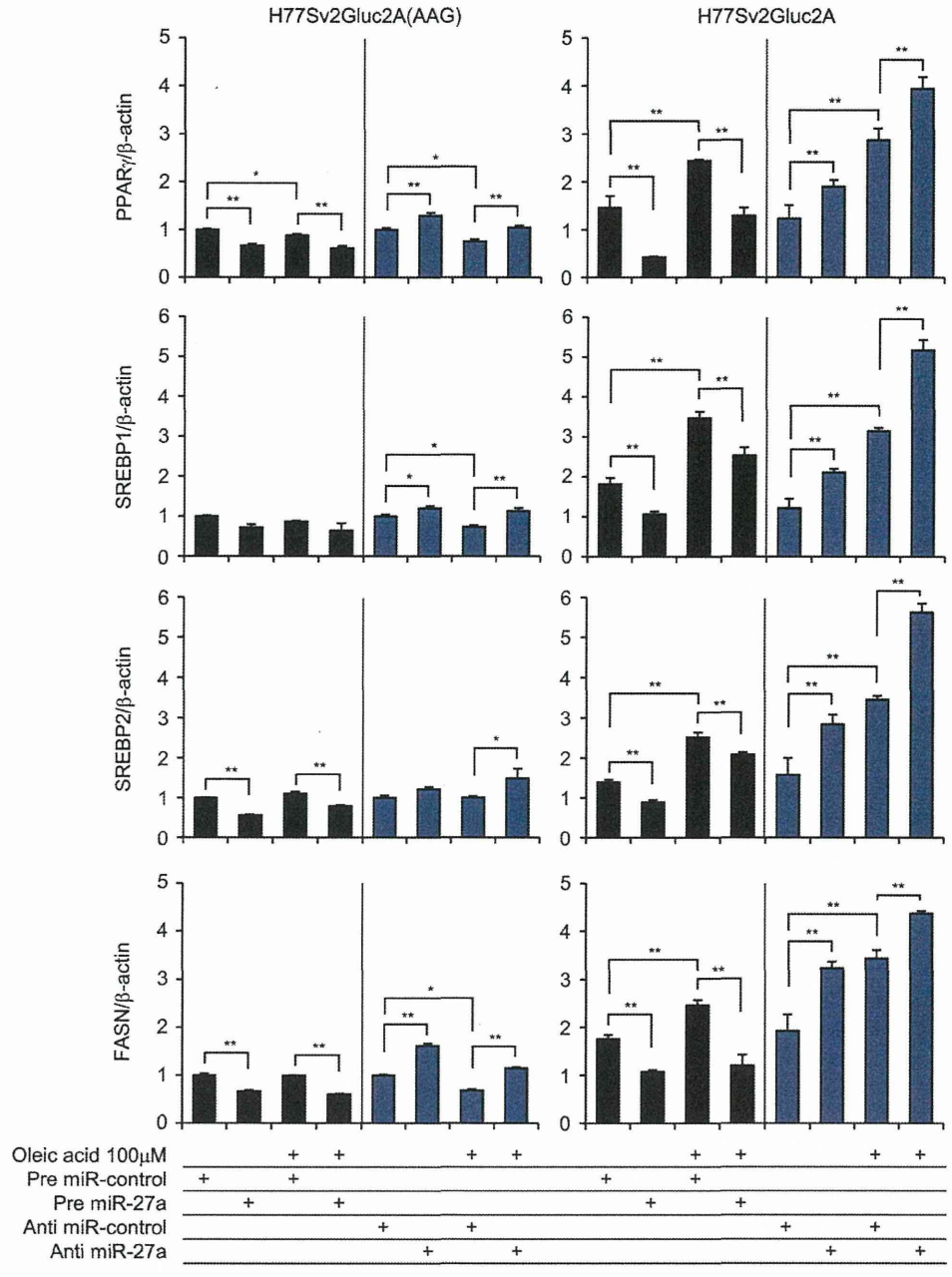

FIG 5 Expression of lipid metabolism-related transcription factors. Huh-7.5 cells were transfected with H77Sv2 Gluc2A RNA or H77Sv2 Gluc2A (AAG) RNA and pre- or anti-miR-27a. At 24 h posttransfection, oleic acid (100 μM) was added to the culture medium, and at 72 h after oleic acid treatment, *PPARγ*, *SREBP1*, *SREBP2*, and *FASN* expression levels were quantified by RTD-PCR ($n = 6$). Experiments were performed in duplicate and repeated three times. Values are means ± standard errors. *, $P < 0.01$; **, $P < 0.005$.

mRNA and protein levels (Fig. 5 and 6A and B). Pre-miR-27a significantly repressed the levels of these transcription factors and, conversely, anti-miR-27a significantly increased their mRNA and protein levels (Fig. 5 and 6A and B). This regulation by miR-27a was observed in both HCV-replicating and non-HCV-replicating cells, although the magnitude of the change was more prominent in HCV-replicating cells (Fig. 5).

As LDs associate with the ER-derived membrane at the site of HCV replication (10) and ER stress was recently shown to promote hepatic lipogenesis and LD formation (31), we next evaluated ER stress markers. Under HCV replication and lipid overload with oleic acid, anti-miR-27a increased the expression of the ER stress markers p-PERK, p-eIF2α, and BiP in Huh-7.5 cells. Conversely, pre-miR-27a significantly decreased the expression of these markers (Fig. 6C). Cell viability decreased after anti-miR-27a transfection and increased following pre-miR-27a treatment (Fig. 6D). Thus, miR-27a repressed the ER stress that was induced by HCV replication and lipid overload.

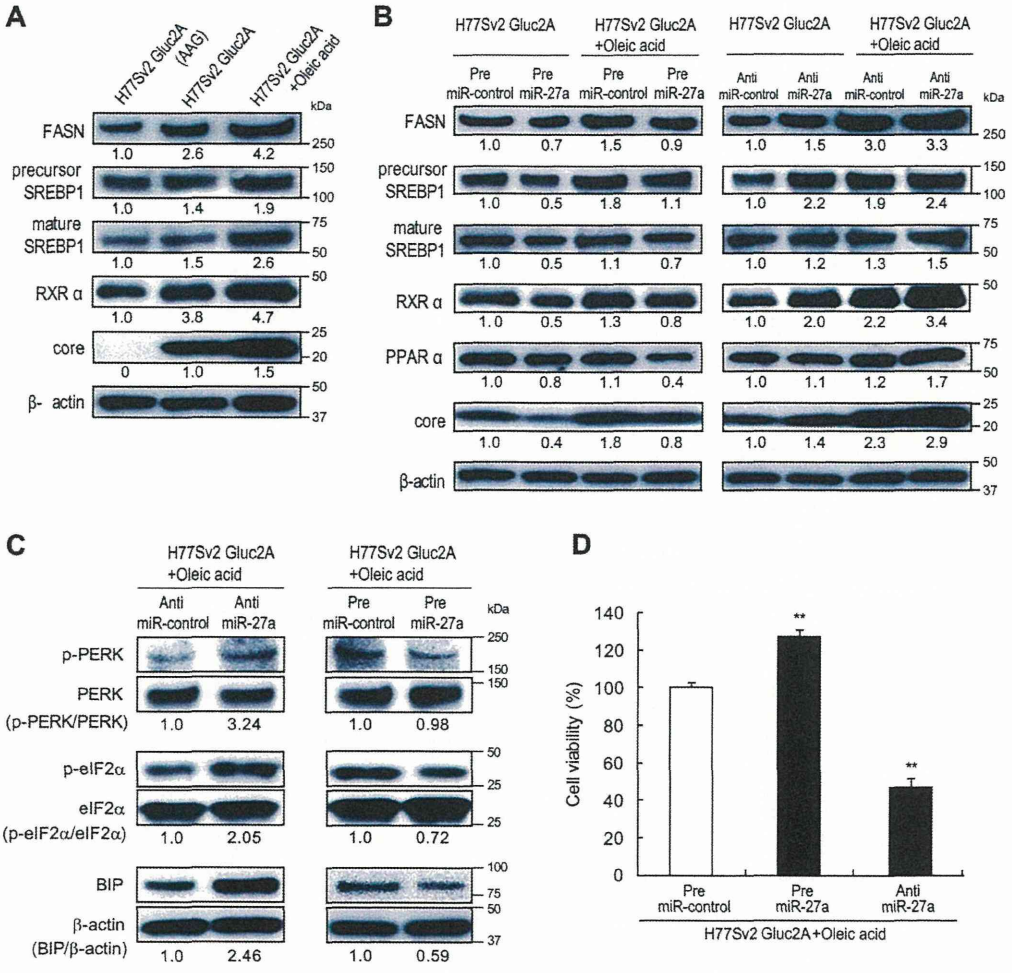

FIG 6 Expression of lipid metabolism-related transcription factors and ER stress-related factors. Huh-7.5 cells were transfected with H77Sv2 Gluc2A RNA or H77Sv2 Gluc2A (AAG) RNA and pre- or anti-miR-27a. At 24 h posttransfection, oleic acid (100 μM) was added to the culture medium. At 72 h after oleic acid treatment, the cells were harvested. (A) Western blotting of lipid metabolism-related transcription factors changed by HCV infection and oleic acid. Experiments were repeated three times. (B) Western blotting of lipid metabolism-related transcription factors changed by pre- or anti-miR-27a. Experiments were repeated three times. (C) Western blotting of ER stress-related transcription factors changed by pre- or anti-miR-27a. Experiments were repeated three times. (D) Cell viability in the same experiments was determined by MTS assay ($n = 9$). Experiments were performed in triplicate and repeated three times. Values are means ± standard errors. *, $P < 0.01$; **, $P < 0.005$.

miR-27a targets RXRα and the ATP-binding cassette transporter ABCA1. We next analyzed the expression of miR-27a target genes. A previous report showed that miR-27a targets RXRα in rat hepatic stellate cells (32), and we confirmed that miR-27a targets the 3′ UTR of human RXRα in Huh-7.5 cells (data not shown). Although the primary sequence of the human RXRα 3′ UTR shares approximately 60% homology with the corresponding rat sequence, the putative miR-27a binding site (ACUGUGAA) is conserved among several different species. Therefore, we constructed an expression vector containing a luciferase (Luc) reporter gene fused to the human RXRα 3′ UTR (pmirGLO-RXRα 3′ UTR) and reevaluated Luc activity (data not shown). Pre-miR-27a repressed Luc activity, while anti-miR-27a significantly increased Luc activity. The introduction of three nucleotide mutations into the conserved miR-27a binding site was shown to abolish these changes in Luc activity. These results confirmed previous findings that miR-27a targets RXRα (32). RXRα interacts with liver X receptor (LXR) and regulates many lipid synthetic genes such as *SREBP1* and *FASN*. We found that the expression of *SREBP1*, *FASN*, and *SREBP2* was regulated by miR-27a (Fig. 6B) and confirmed that *PPARγ* was also regulated by miR-27a, as reported previously (Fig. 5) (33). In addition, *PPARα* was shown to be regulated by miR-27a (Fig. 6B).

We next evaluated the expression of lipid transporter genes. The ATP-binding cassette transporter ABCA1 is mutated in Tangier's disease (34) and plays an important role in the efflux of TCHO for high-density lipoprotein (HDL) synthesis (35). A recent report demonstrated a functional role for ABCA1 in hepatocyte TG secretion to the plasma and in the reduction of cellular TG levels (29). Here we found that pre-miR-27a significantly repressed ABCA1 and, conversely, that anti-miR-27a increased the mRNA and protein levels of ABCA1 (Fig. 7A and B). We identified two miR-27a binding sites (sites 1 and 2) in the 3′ UTR of ABCA1 (Fig. 7C) that were conserved between species (Fig. 7C). An expression vector containing the *luc* reporter gene fused to the human ABCA1 3′ UTR (wild type [WT]) was constructed, and a

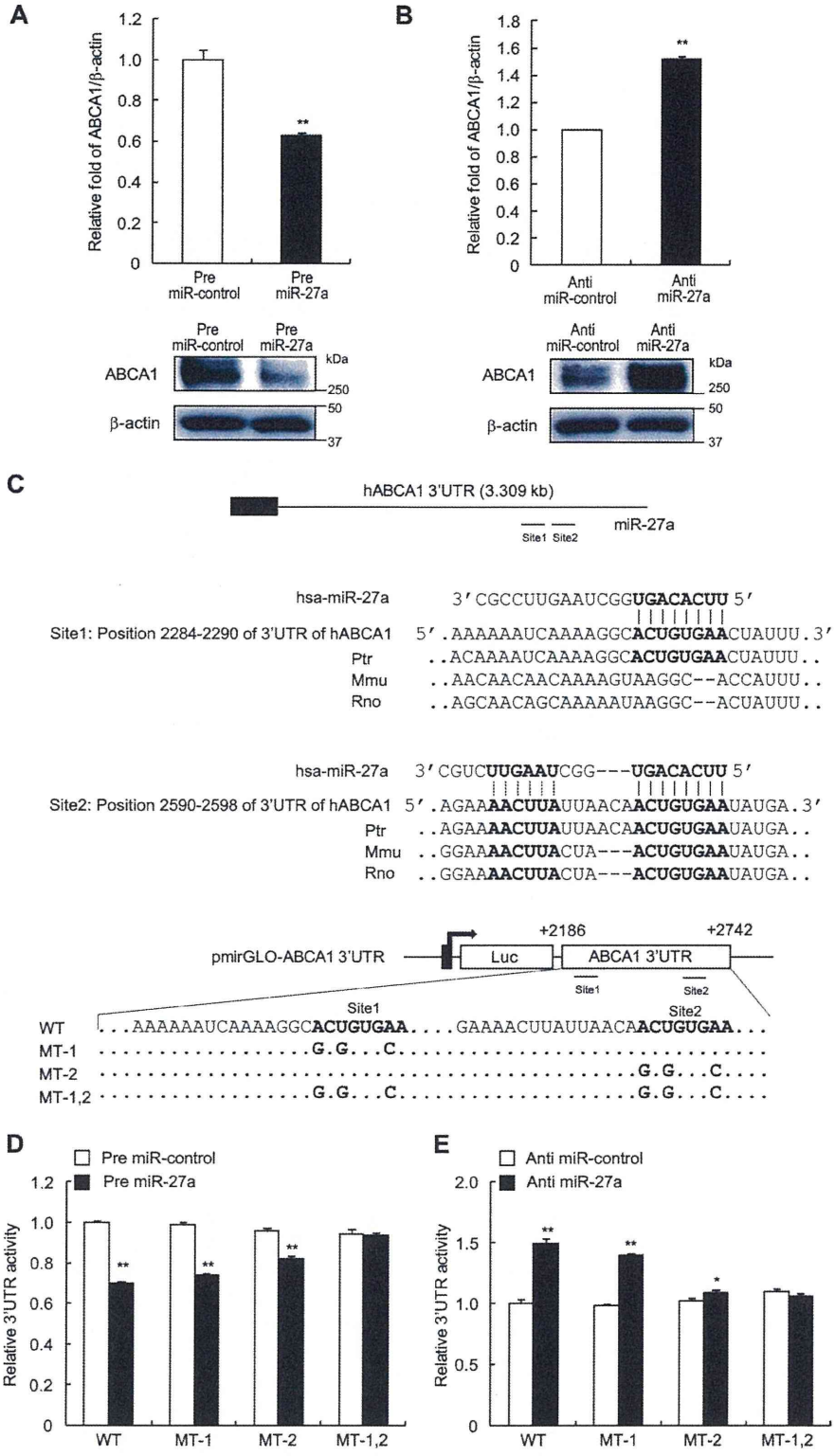

FIG 7 miR-27a targets ABCA1. (A) Regulation of ABCA1 by pre-miR-27a. RTD-PCR and Western blotting of ABCA1 in Huh-7.5 cells at 72 h posttransfection with pre-miR-control and pre-miR-27a ($n = 6$). **, $P < 0.005$. (B) Regulation of ABCA1 by anti-miR-27a. RTD-PCR and Western blotting of ABCA1 in Huh-7.5 cells at 72 h posttransfection with pre-miR-control and anti-miR-27a ($n = 6$). **, $P < 0.005$. (C) Sequence alignment of the ABCA1 3′ UTR and the construction of the luciferase (Luc) expression vector fused to the ABCA1 3′ UTR. Ptr, *Pan troglodytes*; Mmu, *Mus musculus*; Rno, *Rattus norvegicus*; WT, Luc reporter vector with the WT ABCA1 3′ UTR (2186 to 2742); MT-1, Luc reporter vector with the site 1 mutation of the WT; MT-2, Luc reporter vector with the site 2 mutation of the WT; MT-1,2, Luc reporter vector with mutations at sites 1 and 2 of the WT. (D, E) Suppression (D) or induction (E) of Luc activity with the various mutations of the ABCA1 3′ UTR by pre-miR-27a. Huh-7.5 cells were transfected with pre- or anti-miR-control or pre- or anti-miR-27a, and WT, MT-1, MT-2, and MT-1,2. Luc activities were measured at 24 h posttransfection ($n = 6$). All experiments were performed in duplicate and repeated three times. Values are means ± standard errors. *, $P < 0.01$; **, $P < 0.005$.

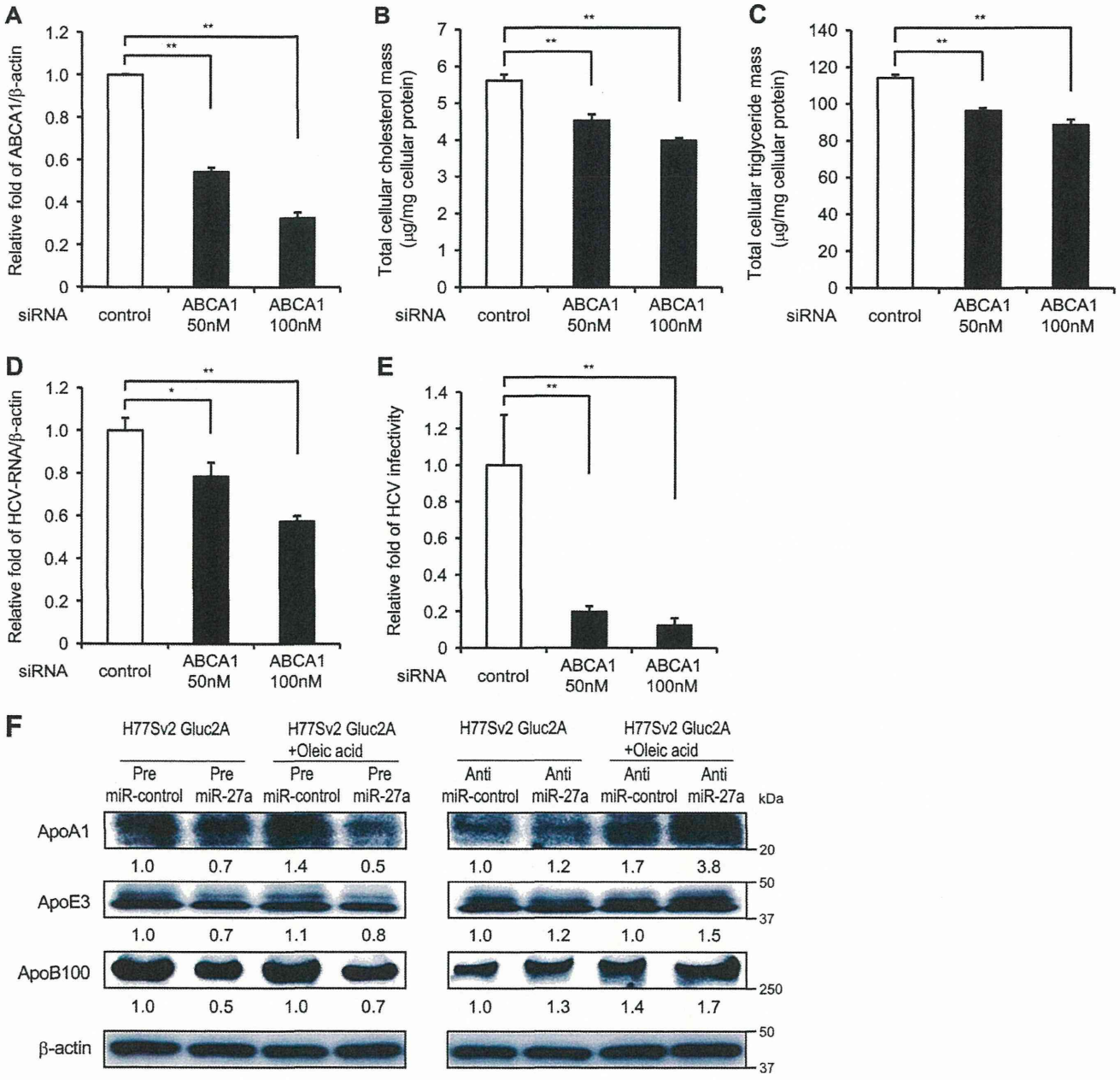

FIG 8 Suppression of ABCA1 inhibits HCV replication and infection. Huh-7.5 cells were transfected with H77Sv2 Gluc2A RNA and siRNA to ABCA1 or control siRNA. ABCA1 expression was quantified at 72 h posttransfection by RTD-PCR ($n = 6$). (A) Knockdown efficiency of ABCA1 in Huh-7.5 cells by siRNA. (B) TG concentration in cells ($n = 6$). (C) TCHO concentrations in cells ($n = 6$). (D) HCV RNA assay by RTD-PCR ($n = 6$). (E) HCV infectivity. Huh-7.5 cells were infected with HCVcc derived from ABCA1 knockdown Huh-7.5 cells. HCV RNA was quantified at 72 h postinfection by RTD-PCR ($n = 6$). Experiments were performed in duplicate and repeated three times. Values are means ± standard errors. *, $P < 0.01$; **, $P < 0.005$. (F) Regulation of ApoA1, ApoE2, and ApoB100 by miR-27a. Experiments were performed under the same conditions as Fig. 6B and C and repeated three times.

series of mutations were introduced into the putative miR-27a binding sites (MT-1, MT-2, and MT-1,2). The Luc activity of the WT was significantly repressed by pre-miR-27a and increased by anti-miR-27a. However, there was a smaller change in Luc activity caused by pre- and anti-miR-27a in the single mutants (MT-1 and MT-2) and no change in Luc activity in the double mutant (MT-1,2) (Fig. 7D and E). These results show that miR-27a targets ABCA1 to decrease the lipid content of cells.

The functional relevance of ABCA1 in lipid metabolism and HCV replication in Huh-7.5 cells was examined by inhibiting ABCA1 with an siRNA (Fig. 8). siRNA to ABCA1 repressed the expression of ABCA1 in a dose-dependent manner (Fig. 8A). Under this condition, the cellular TG and TCHO levels decreased significantly (Fig. 8B and C) and HCV RNA levels also decreased to 57% of the control. More strikingly, HCV infectivity decreased to 12% of the control (Fig. 8D and E).